

PAPER • OPEN ACCESS

## Indium Antimonide Based Terahertz Plasmonic Ring Resonator Filter

To cite this article: Sherin Thomas and M.N. Satyanarayan 2023 *J. Phys.: Conf. Ser.* **2426** 012012

View the [article online](#) for updates and enhancements.

You may also like

- [Pulsed terahertz tomography](#)  
S Wang and X-C Zhang
- [Photonic terahertz technology](#)  
Alvydas Lisauskas, Torsten Löffler and Hartmut G Roskos
- [Random Frequency Accessible Broad Tunable Terahertz-Wave Source Using Phase-Matched 4-Dimethylamino-N-methyl-4-stilbazolium Tosylate Crystal](#)  
Hiromasa Ito, Koji Suizu, Tomoyu Yamashita et al.



The banner features a teal background on the left with the ECS logo and meeting details. On the right, a vibrant image shows silhouettes of people in a modern, sunlit setting with a network overlay.

**ECS** 244th ECS Meeting  
Gothenburg, Sweden • Oct 8 – 12, 2023  
Register and join us in  
advancing science!  
Learn More & Register Now!

# Indium Antimonide Based Terahertz Plasmonic Ring Resonator Filter

Sherin Thomas and M.N.Satyanarayan

Optoelectronics Laboratory, Department of Physics, National Institute of Technology  
Karnataka, Surathkal, Mangalore – 575025, INDIA

E-mail: [satya\\_mn@nitk.edu.in](mailto:satya_mn@nitk.edu.in)

**Abstract.** This paper proposes a tunable filter composed of a semiconductor-insulator-semiconductor (SIS) waveguide with a ring resonator at terahertz (THz) frequency. The two-dimensional study of the proposed structure has been done using the finite element method. It is observed that the device can be used for filtering THz frequency within the range of 0.4 THz to 0.9 THz by varying the structural parameters. The simulated structure is a promising candidate for an integrated optical circuit and terahertz devices as a filter. The results of the simulations are discussed in detail.

## 1. Introduction

The well flourished micro and nanofabrication technology and the theoretical knowledge are driving the innovations in the designed structure system. This provides useful electromagnetic and optical properties. The research community is getting attracted to the manipulation of electromagnetic properties of different structural designs on different materials. This includes a wide variety of interdisciplinary applications such as plasmonics, photonics, biosensors, etc [1]. Plasmonics is one of the attractive fields in which the electromagnetic response of metallic and semiconductor systems is studied. Focusing and confining the electromagnetic waves to the subwavelength dimension is the most interesting feature observed in plasmonic systems [2]. When the metals are excited with electromagnetic radiations of frequency lesser than the plasma frequency, free electrons gas behavior comes into the picture. This leads to the collective oscillation of free electrons on the surface, basically the surface waves. When this surface wave resonates with the external electromagnetic wave, the surface plasmon polaritons (SPP) are produced. Materials that show metal-like properties in the terahertz (THz) regime can support SPPs at THz frequencies [3].

Plasmonic waveguides are attractive because of the confinement of electromagnetic energy at the metal-dielectric interface. Usually, waveguides are electromagnetic waveguiding structures with reduced loss. In the initial days, plasmonic waveguides emerged as the alternative to conventional dielectric waveguides. The topology of the metal surface determines the propagation of 2D electromagnetic wave modes with limited propagation length [4].

Plasmonic devices have different kinds of applications such as filters [5], absorbers [6], splitters [7] and sensors [8]. Among these, sensors have got good attention because of their size and compatibility compared with fiber sensors and other silicon-based sensors. Here, in the sensing field, plasmonic resonating structures have been studied due to their tunability. By changing



the structural dimensions, it is possible to change the resonance frequency thereby sensing. There are different types of resonating structures. In that, ring and stub resonators are of great interest because of their simplicity in structure and good sensitivity in resonance. Zang et al. proposed plasmonic refractive index sensors using concentric ring resonators associated with a bus waveguide achieving a sensitivity around 1060 nm/refractive index unit. This waveguide and the resonating structures are designed on a silver surface and the resonating wavelengths are a few micro-meters [9].

Over the past decades, the scientific community got attracted to terahertz technology by the wide variety of its applications such as THz imaging [10], biomolecule sensing [11], nondestructive testing [12], and communication [13]. To fulfill these applications, efficient and well-functioning devices are designed based on plasmonics and metamaterials in the range of 0.1 to 10 THz [14].

This paper introduces a frequency filter composed of a straight waveguide and a ring resonator in the terahertz frequency regime. Microring resonators and optical ring resonators are well explored by researchers but terahertz ring resonators are not studied well. Thus, we present a THz frequency filter that works between 0.4 to 0.9 THz. The frequency tuning is achieved by varying the structural parameters.

## 2. Device modeling and analysis

The basic plasmonic waveguides are composed of metals and insulators. This metal-insulator-metal waveguide shows the response in the visible and IR frequency spectrum [15]. Semiconductors that have a negative real part of permittivity can support SPP propagation through the semiconductor-insulator interface. Among the semiconductors, indium antimonide (InSb) shows a better response toward SPP at THz frequencies [16].

Figure 1 represents the designed filter structure, which is composed of Air and Indium antimonide (InSb). The structural parameters  $R$ ,  $W$ , and  $g$  are the radius of the outer ring, the width of the waveguide, and the space between the ring resonator and the straight waveguide respectively. The InSb takes complex relative permittivity values at different frequencies according to the Drude model [17].

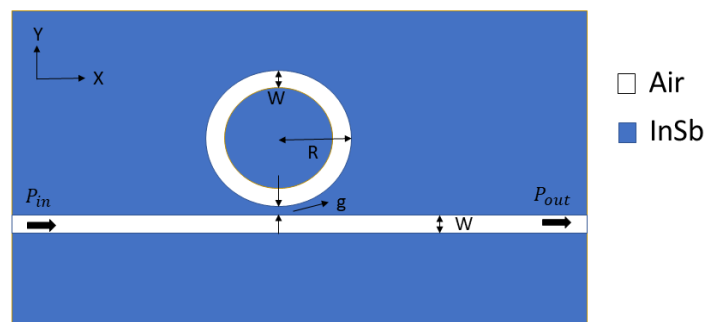


Figure 1: Designed filter structure with straight waveguide and ring resonator with parameters  $w=40$   $\mu\text{m}$ ,  $R=90$   $\mu\text{m}$ , and  $g=2$   $\mu\text{m}$ .

$$\epsilon(\omega) = \epsilon_{\infty} - \frac{\omega_p^2}{(\omega^2 + i\gamma\omega)} \quad (1)$$

where  $\epsilon_{\infty}$  is the high frequency permittivity. It is a constant for the material medium. For InSb  $\epsilon_{\infty}=15.6$ .  $\omega$  is the working frequency and  $\gamma$  is the damping coefficient of the material.  $\omega_p$  is also

a material property called the plasma frequency and it is defined by the equation. [18]

$$\omega_p = \sqrt{\frac{Ne^2}{m_e \epsilon_0}} \quad (2)$$

$\omega_p$  depends on the number of free electrons of the material  $N$ , charge of electron  $e$ , effective mass of electron  $m_e$ , and the permittivity of free space  $\epsilon_0$ . The frequency dependent permittivity of indium antimonide at 0.7 THz is  $-101.75+i6.808$  and the relative permittivity of air is one.

The transmission study for the above device has been done with dimensions  $R=90$   $\mu\text{m}$ ,  $W=40$   $\mu\text{m}$ , and  $g=2$   $\mu\text{m}$  is given in figure 2. COMSOL Multiphysics is the simulation tool that works on the finite element method (FEM). All the boundaries in the simulation domain are treated as perfect electric conductors and an electromagnetic wave frequency domain study have performed. The maximum power is obtained when the width of the waveguide matches the width of the ring resonator.

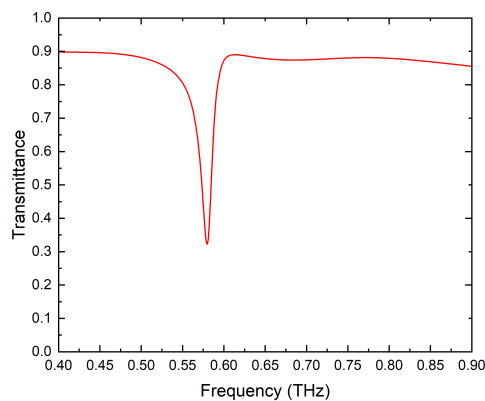


Figure 2: Frequency response of ring resonator with  $w=40$   $\mu\text{m}$ ,  $R=90$   $\mu\text{m}$ , and  $g=2$   $\mu\text{m}$ .

The incident and transmitted power are measured by two power monitors  $P_{in}$  and  $P_{out}$ . Hence the transmittance is given by  $T = \frac{P_{out}}{P_{in}}$ . The transmission of the device is studied in the range of 0.4 to 0.9 THz frequency.

The frequency coupling of the ring resonator at the resonance frequency is given in equation 3. [9],

$$N\lambda = Re(n_{eff})L_{eff} \quad (3)$$

Resonance wavelength  $\lambda$  depends on the effective index of the medium  $n_{eff}$  and the effective path length  $L_{eff}$ , which can be found by taking the average of the inner and outer perimeter of the ring. In equation 3  $N$  is an integer that represents the mode number. At the resonance frequency, transmitted power will be limited or lowered to zero. From figure 2 the resonance frequency of the ring resonator of dimension  $w=40$   $\mu\text{m}$ ,  $R=90$   $\mu\text{m}$ , and  $g=2$   $\mu\text{m}$  is 0.58 THz.

The background mechanism of the ring resonator can be found by studying the field distribution through the device. Figure 3 shows the field distribution inside the ring resonator at a resonating and a non-resonating frequency. At the resonance frequency transverse magnetic ( $\text{TM}_1$ ) wave got coupled to the ring resonator and the majority of the field got confined in the ring. Then less amount of field coupled back to the straight waveguide results in a lower transmission. At a non-resonating frequency, the whole signal gets coupled back to the straight waveguide.

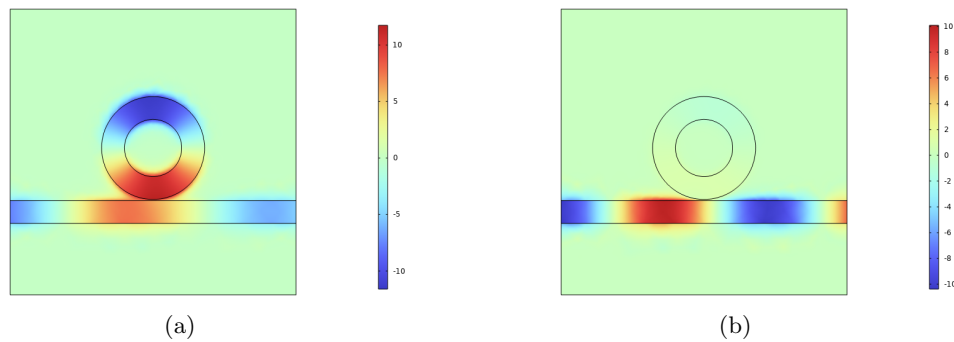


Figure 3: (a) z component of magnetic field ( $H_z$ ) at 0.58 THz (resonating frequency) (b)  $H_z$  at a at 0.7 THz (a non resonating frequency).

### 3. Geometric parameters evaluation

The main parameter that is directly related to the resonance frequency is the ring radius. The effective path length of the device will add up by increasing the outer radius of the ring resonator. As a result, the resonance frequency gets shifted to the left side of the frequency band and it is shown in figure 4(a)[19]. The resonance frequency values for different outer radii are plotted in figure 4(b) and it shows a linear behavior. It is important to study the full width at half maximum (FWHM) values of the device for these different radius values because it decides the filter's quality factor (Q) [20]. The quality factor is calculated by equation 4 [21].

$$Q = \frac{f}{FWHM} \quad (4)$$

where  $f$  is the resonance frequency and  $FWHM$  is the full width at half maximum for the resonance frequency. By varying the R values starting from 80um to 100um the FWHM takes values of 0.0133, 0.0115, 0.0105, 0.0094, and 0.0092 THz respectively. We obtained a maximum quality factor of 63 for an outer radius value (R) of 95um.

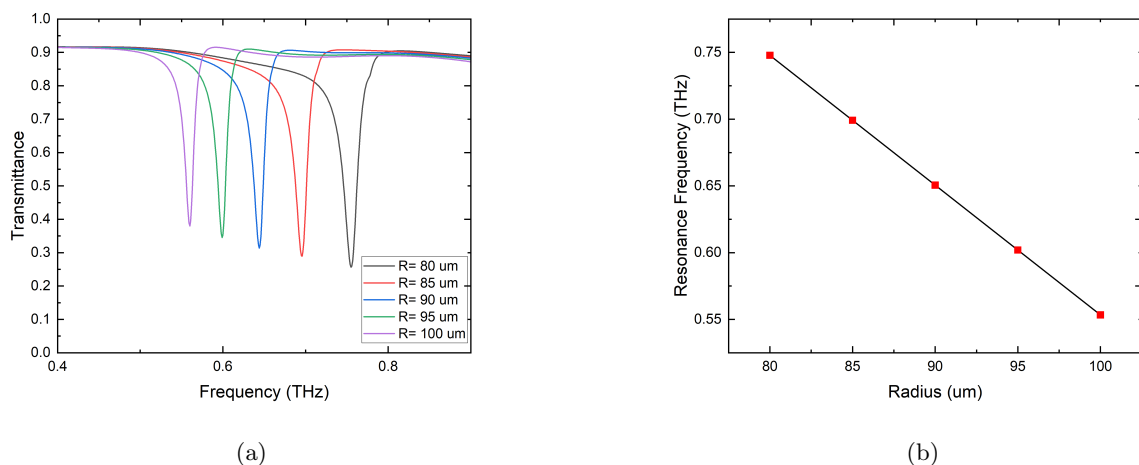


Figure 4: (a) Transmission corresponds to different values of outer radii. (b) Variation of resonance frequency with change in outer radii.

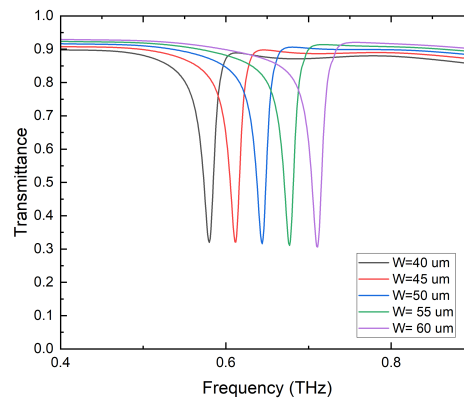


Figure 5: Transmission corresponds to different values of the width of the waveguide.

The frequency selection is achieved by changing the width of the waveguide.  $L_{eff}$  will decrease by increasing the width by keeping the outer ring radius the same. As a result, the resonance frequency gets shifted to the right side of the frequency band as shown in figure 5. The FWHM values are varying between 0.0108 THz and 0.0095 THz. A maximum Q value of 70 has been obtained by changing the width of the straight waveguide. The shift in resonance frequency values is less as compared with that figure 4. But without affecting the transmittance much, it is possible to change the resonance frequency values. These studies show, the investigated structure can be treated as a THz frequency filter and can be used for different THz applications.

#### 4. Conclusion

In conclusion, the transmission spectrum associated with a ring resonator coupled with an SIS waveguide is studied in detail. The device can be used as a THz frequency filter that works within the frequency range of 0.4 THz to 0.9 THz. The tuning of the proposed filter can be done by varying the geometrical parameters. Hence the designed device is a promising candidate for THz circuits and also can be used for sensing.

#### References

- [1] Ozbay E 2006 *science* **311** 189–193
- [2] Berweger S, Atkin J M, Olmon R L and Raschke M B 2012 *The Journal of Physical Chemistry Letters* **3** 945–952
- [3] Kong F, Li K, Huang H, Wu B I and Kong J 2008 *Progress In Electromagnetics Research* **82** 257–270
- [4] Han Z and Bozhevolnyi S I 2012 *Reports on Progress in Physics* **76** 016402
- [5] Wu W, Yang J, Zhang J, Huang J, Chen D and Wang H 2016 *Optics letters* **41** 2310–2313
- [6] Wu D, Liu C, Liu Y, Yu L, Yu Z, Chen L, Ma R and Ye H 2017 *Optics letters* **42** 450–453
- [7] Yu Y, Si J, Ning Y, Sun M and Deng X 2017 *Optics letters* **42** 187–190
- [8] Chen L, Liu Y, Yu Z, Wu D, Ma R, Zhang Y and Ye H 2016 *Optics express* **24** 9975–9983
- [9] Zhang Z, Yang J, He X, Zhang J, Huang J, Chen D and Han Y 2018 *Sensors* **18** 116
- [10] Dean P, Valavanis A, Keeley J, Bertling K, Lim Y, Alhathloul R, Burnett A, Li L, Khanna S, Indjin D *et al.* 2014 *Journal of Physics D: Applied Physics* **47** 374008
- [11] Hong J, Jun S, Cha S, Park J, Lee S, Shin G and Ahn Y 2018 *Scientific reports* **8** 1–8

- [12] Tao Y H, Fitzgerald A J and Wallace V P 2020 *Sensors* **20** 712
- [13] Song H J and Nagatsuma T 2011 *IEEE transactions on terahertz science and technology* **1** 256–263
- [14] Huang L, Chen X, Mühlenbernd H, Zhang H, Chen S, Bai B, Tan Q, Jin G, Cheah K W, Qiu C W *et al.* 2013 *Nature communications* **4** 1–8
- [15] Dionne J, Sweatlock L, Atwater H and Polman A 2006 *Physical Review B* **73** 035407
- [16] Giannini V, Berrier A, Maier S A, Sánchez-Gil J A and Rivas J G 2010 *Optics express* **18** 2797–2807
- [17] Taliercio T and Biagioni P 2019 *Nanophotonics* **8** 949–990
- [18] Maier S A *et al.* 2007 *Plasmonics: fundamentals and applications* vol 1 (Springer)
- [19] Holmgaard T, Chen Z, Bozhevolnyi S I, Markey L and Dereux A 2009 *Optics express* **17** 2968–2975
- [20] Madadi Z, Abedi K, Darvish G and Khatir M 2019 *Optik* **183** 670–676
- [21] Hajshahvaladi L, Kaatuzian H and Danaie M 2019 *Optical and Quantum Electronics* **51** 1–16